Quaternary Science Reviews 196 (2018) 118–123

Contents lists available at ScienceDirect

Quaternary Science Reviews

journal homepage: www.elsevier.com/locate/quascirev

Rapid Laurentide ice-sheet advance towards southern last glacial maximum limit during marine isotope stage 3

Anders E. Carlson [a, *], Lev Tarasov [b], Tamara Pico [c]

[a] College of Earth, Ocean, and Atmospheric Sciences, Oregon State University, USA
[b] Department of Physics and Physical Oceanography, Memorial University, Canada
[c] Department of Earth and Planetary Sciences, Harvard University, USA

ARTICLE INFO

Article history:
Received 21 February 2018
Received in revised form
23 April 2018
Accepted 29 July 2018
Available online 7 August 2018

ABSTRACT

Marine isotope stage (MIS) 3 (~58–28 ka) is a period of intermediate global ice volume between MIS 4 and the last glacial maximum of MIS 2. Here we report geologic evidence for southern Laurentide ice-sheet rapid growth to near its last glacial maximum extent after a period with limited ice in the southernmost Hudson Bay lowland. A ^{14}C age on wood in lacustrine sediments interbedded with glacial tills in central-eastern Wisconsin dates a Laurentide ice-sheet advance southwards to an extent at least equivalent to at least its ~17 ka deglacial limit by 39.1 ± 0.4 ka. This advance ended before 30.4 ± 0.9 ka based on another ^{14}C date on wood in lacustrine sediment overlying the till layers. This advance is consistent with ^{14}C ages from Michigan and Iowa, and Gulf of Mexico runoff records that support a concurrent southern Laurentide ice-sheet advance. We infer changes in North American ice volume using ice-sheet model simulations from a large ensemble that are consistent with ^{14}C-data and Gulf of Mexico-discharge constraints. The simulations show the Laurentide ice sheet growing from a volume equivalent to 25–30 m of global mean sea level (GMSL) before ~40 ka to 40–45 m of GMSL at ~40 ka, and reaching 65–70 m GMSL by ~30 ka, consistent with glacial isostatic adjustment assessments of near-to intermediate-field sea-level data. We thus show from our terrestrial field data and ice-sheet model simulations that an individual ice sheet can grow rapidly, which has only been inferred previously for global ice volume from GSML records.

1. Introduction

Following a relative 'glacial' period during marine isotope stage (MIS) 4 (~68–58 ka), the globe entered the 'interglacial' period of MIS 3 (~58–28 ka) (e.g., Lisiecki and Stern, 2016). Significant ice volume remained in boreal latitudes during MIS 3 that then expanded to its last glacial maximum (LGM) during MIS 2 (e.g., Clark et al., 1993, 2009; Dyke et al., 2002; Stokes et al., 2012; Lambeck et al., 2014). A summary of benthic δ^{18}O and relative sea-level records by Siddall et al. (2008) suggested a global terrestrial ice volume relative to present during MIS 3 that was equivalent to an ~60–80 m fall in global-mean sea level (GMSL), which agrees with Lambeck et al. (2014). In contrast, a recent glacial isostatic adjustment (GIA) analysis of sea-level indicators in the Bohai Sea and the U.S. mid-Atlantic suggested a MIS 3 GMSL highstand of approximately −38 m during the time interval 50–35 ka (Pico et al., 2016, 2017).

Dalton et al. (2016) recently argued for ice-free conditions in the southernmost Hudson Bay lowland during MIS 3 prior to ~40 ka based on finite accelerator mass spectrometry (AMS) ^{14}C ages (Fig. 1) and other chronologic constraints, with ice-free conditions extending further to the south (e.g., Bajc et al., 2015). This agrees with earlier interpretations of Thorleifson et al. (1992) of glacial-lacustrine sediments between an LGM till and an older till unit, and other studies that lacked more precise direct chronologic controls on the glacial-lacustrine unit (e.g., Skinner, 1973; Dredge and Thorleifson, 1987; Allard et al., 2012; Dubé-Loubert et al., 2013). Farther north, such proglacial/interglacial sediments are lacking, implying continued ice cover of the central to northern Hudson Bay lowland during MIS 3 (e.g., Nielsen et al., 1986; Dredge et al., 1990; Thorleifson et al., 1992; Roy, 1998; Carlson et al., 2004). After this retracted ice interval of mid MIS 3, Dyke et al. (2002) estimated Laurentide ice-sheet extent during late MIS 3 with an ice margin roughly following the outline of the Canadian Shield.

* Corresponding author.
E-mail address: acarlson@coas.oregonstate.edu (A.E. Carlson).

https://doi.org/10.1016/j.quascirev.2018.07.039
0277-3791/

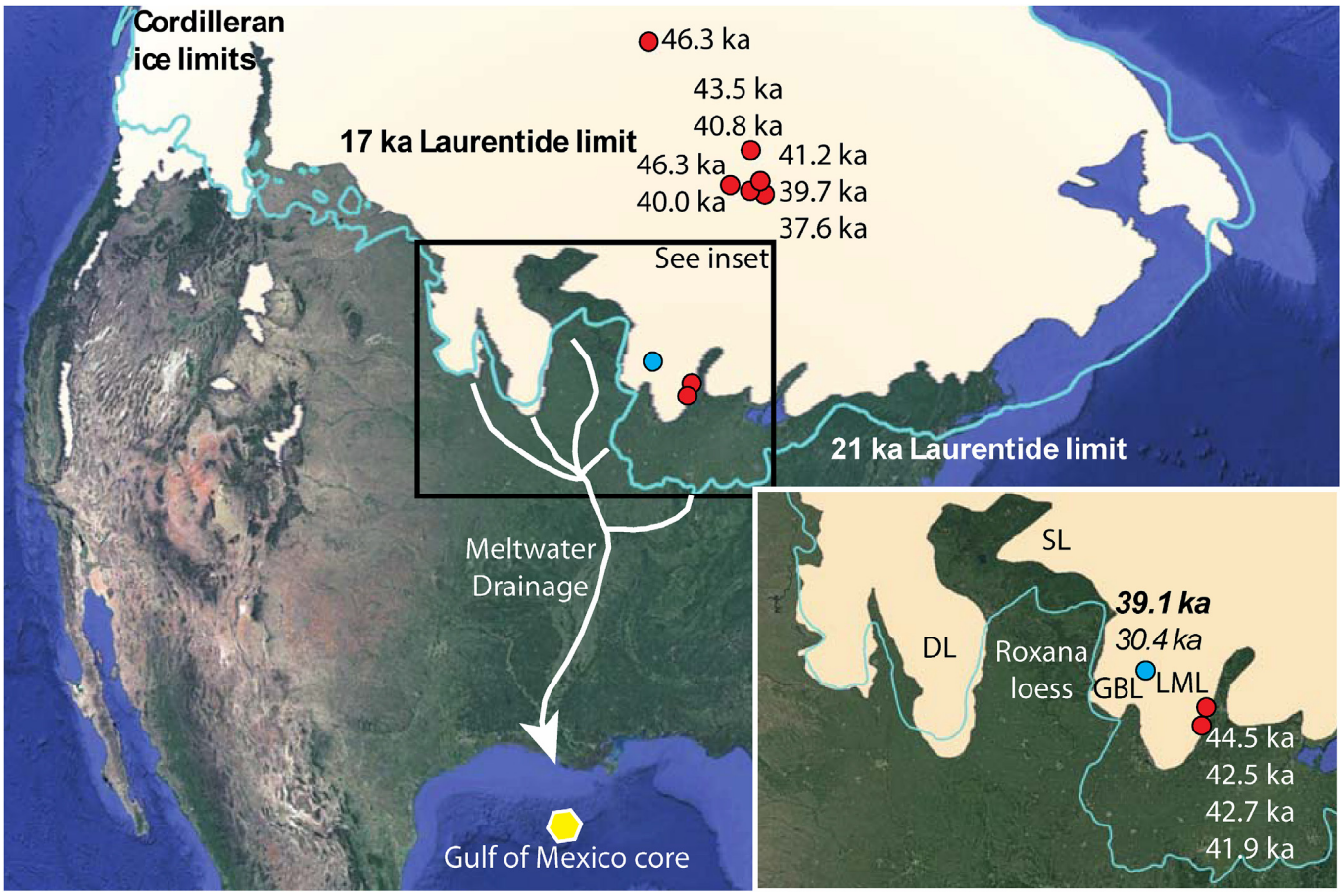

Fig. 1. Map of the 17 ka (tan) and 21 ka (blue line) of the Laurentide ice sheet (Dyke, 2004). Red circles indicate finite AMS ^{14}C ages; blue circle is the AMS ^{14}C dates that constrain advance and retreat of the Laurentide in Wisconsin. Meltwater drainage path to the Gulf of Mexico $\delta^{18}O_{sw}$ record (yellow hexagon) is delimited. Inset shows the Lake Michigan (LML), Green Bay (GBL), Superior (SL) and Des Moines (DL) lobes, with AMS radiocarbon dates indicated (bold italic is age of advance; italic is age of retreat). Location of the Roxana loess is noted (e.g., Syverson and Colgan, 2011; Muhs et al., 2018). (For interpretation of the references to color in this figure legend, the reader is referred to the Web version of this article.)

Uncertainties in ice-sheet extent prior to the LGM are largely due to the destruction of glacial evidence by advancing ice during MIS 2 as well as the limitation of dating techniques (Clark et al., 1993; Dyke et al., 2002; Kleman et al., 2010; Syverson and Colgan, 2011; Stokes et al., 2012; Hughes et al., 2015). The growth of ice-sheet volume towards the LGM is also poorly constrained prior to ~26 ka and would require rapid growth of ice during the latter part of MIS 3 to fit the GMSL fall from approximately −38 m at ~44 ka to approximately −130 m at the LGM (<26 ka; Clark et al., 2009; Austermann et al., 2013; Lambeck et al., 2014) proposed in the model of Pico et al. (2017). Rapid growth of global ice volume has previously been inferred from far-field sea-level indicators (e.g., Clark et al., 2009; Lambeck et al., 2014), but has yet to be assessed at an individual ice-sheet scale. The one exception is the Eurasian ice sheets, which contained <6 m of GMSL across this time period (Hughes et al., 2015). Consequently, GMSL changes during MIS 3 were likely driven by changes in North American and/or Antarctic ice-sheet volume.

Here we discuss evidence for a MIS 3 Laurentide ice-sheet advance in Wisconsin that is ^{14}C dated by AMS (Fig. 1). We use these new age constraints to identify North American ice-sheet model simulations that match the geologic record, and document North American ice-sheet evolution across the latter part of MIS 3. Our findings suggest that at least the southern Laurentide ice sheet advanced to near its LGM extent well prior to the classically defined LGM of 26–19 ka (Clark et al., 2009).

2. Plymouth, Wisconsin glacial sediments

Four rotosonic industry boreholes were drilled in 1999 to examine groundwater contamination from a landfill near Plymouth, Wisconsin (43.75°N, 87.98°W). We were allowed to collect limited samples from the boreholes and describe the units (see Carlson et al., 2011). Additional sampling was not allowed by the industry contractor. Two of the boreholes extended to bedrock with the longest sampling ~100 m of sediment above bedrock. Below the LGM glacial till (the New Berlin till; ~65 m thick) is a sequence of lacustrine sediment (~15 m thick) that is underlain by three till layers interbedded with proglacial silts, sands and gravels (combined thickness of ~24 m). The lower till layers were reddish-gray and had 34–50% sand, 30–46% silt and 15–26% clay content. This lowest glacial unit rests upon dolomite bedrock and was informally named the Plymouth tills (Carlson et al., 2011). An AMS ^{14}C age on wood (*Fagus*) from a silt layer interbedded between the two lower Plymouth till units dates the till layers to 39.1 ± 0.4 ka (34.61 ± 0.39 ^{14}C ka; Beta-129847). Another AMS ^{14}C age on wood (unidentified) from the lacustrine sequence above the three Plymouth tills dates the end of till deposition to before 30.4 ± 0.9 ka (26.40 ± 0.92 ^{14}C ka; OS-24520). These ^{14}C dates were calibrated with IntCal13; reported uncertainties for these dates and other dates discussed below are 1 sigma.

The location of these glacial till layers is within the LGM extent of the Lake Michigan lobe of the Laurentide ice sheet suggesting

that they were deposited by a MIS 3 advance of this lobe southward through the Lake Michigan basin (Fig. 1). The Plymouth site was ice-free by ~17 ka during the last deglaciation (Attig et al., 1985; Maher and Mickelson, 1996; Dyke, 2004; Ullman et al., 2015), suggesting a Laurentide ice-sheet advance in eastern Wisconsin by ~39 ka equivalent to at least its ~17 ka deglacial extent (Fig. 1). Other tills below the LGM New Berlin till are found in central-eastern Wisconsin but are not dated, confounding the further refinement of the extent of this MIS 3 glacial advance (Carlson et al., 2011).

3. Ice-sheet model simulations

We utilize the ensemble of North American ice-sheet model simulations of Tarasov et al. (2012) that were discussed in Stokes et al. (2012) to convert our inferred extent of the southern Laurentide ice sheet into GMSL. These simulations were forced by a climate index approach, scaling a weighted average of the LGM climate anomalies from PMIP II general circulation climate models relative to present-day climate using a Greenland ice-core based index (Tarasov et al., 2012). For the pre-LGM, the climate forcing was temporally modified to better fit the general evolution of GMSL (Stokes et al., 2012). We sieve this ensemble of glacial-cycle simulations to identify those that have ice-free conditions in the southernmost Hudson Bay lowland when indicated by AMS ^{14}C ages (Figs. 1 and 2a) (Dalton et al., 2016), and a subsequent ice advance to cover the Plymouth tills site and the AMS ^{14}C ages in Michigan from below pre-LGM till (summarized by Colgan et al., 2015) (Figs. 1 and 2a). We also extract from these simulations the meltwater discharge down the Mississippi River to the Gulf of Mexico to compare with a Gulf of Mexico $\delta^{18}O_{sw}$ runoff record (Hill et al., 2006) (Figs. 2b and 3). We do not convert changes in $\delta^{18}O_{sw}$ into changes in meltwater discharge (e.g., Carlson, 2009) as the Laurentide δ^{18}O-ice end member likely changed across these multi-millennial timescales (e.g., Vetter et al., 2017).

We considered eight simulations from the North American ice-sheet-complex ensemble of ten thousand simulations (Stokes et al., 2012; Tarasov et al., 2012) that best fit the above-mentioned chronologic constraints (Figs. 1 and 4b, c) and that also perform reasonably well against LGM and deglacial geological data (relative sea level, marine limit, present-day vertical velocities, lake strand lines, ice-margin chronology) as discussed in Tarasov et al. (2012) and Stokes et al. (2012). The North American ice-volume evolution (in m GMSL) of these simulations is shown in Fig. 2c while the area/thickness of one simulation (ID 5919) is shown in Fig. 4b (44 ka) and Fig. 4c (40 ka).

Comparison of the resulting simulated meltwater discharge to the Gulf of Mexico with the Hill et al. (2006) Gulf of Mexico $\delta^{18}O_{sw}$ record based on *Globigerinoides ruber* (pink) (Fig. 3a), which lives in the summer, identifies two of the eight simulations that best agree with the geologic record. While all eight simulations have meltwater events to the Gulf of Mexico, only simulations 5919 and 5939 agree in timing with the decreases in $\delta^{18}O_{sw}$ that Hill et al. (2006) interpreted to mainly reflect southern Laurentide ice-sheet meltwater discharge down the Mississippi River to the Gulf of Mexico (e.g., Kennett and Shackleton, 1975; Leventer et al., 1982; Hill et al., 2006; Carlson, 2009; Williams et al., 2012; Wickert et al., 2013; Wickert, 2016; Vetter et al., 2017). Specifically, these two simulations show increased meltwater discharge of 0.08–0.18 Sv (Sverdrups, 10^6 m^3 s^{-1}) (Fig. 3b and c) during the three meltwater events centered on 39–38 ka, 33–32 ka and ~29 ka (Fig. 3a). 5939 contains another discharge event at 36–35 ka that is not observed in the smoothed Gulf of Mexico $\delta^{18}O_{sw}$ record (Fig. 3a). The raw record does show a $\delta^{18}O_{sw}$ decrease at ~35 ka, but this is defined by a single data point (Fig. 3a). Both model simulations have two peaks in discharge between ~34 ka and ~32 ka whereas the $\delta^{18}O_{sw}$ record has a broader single peak (Fig. 3).

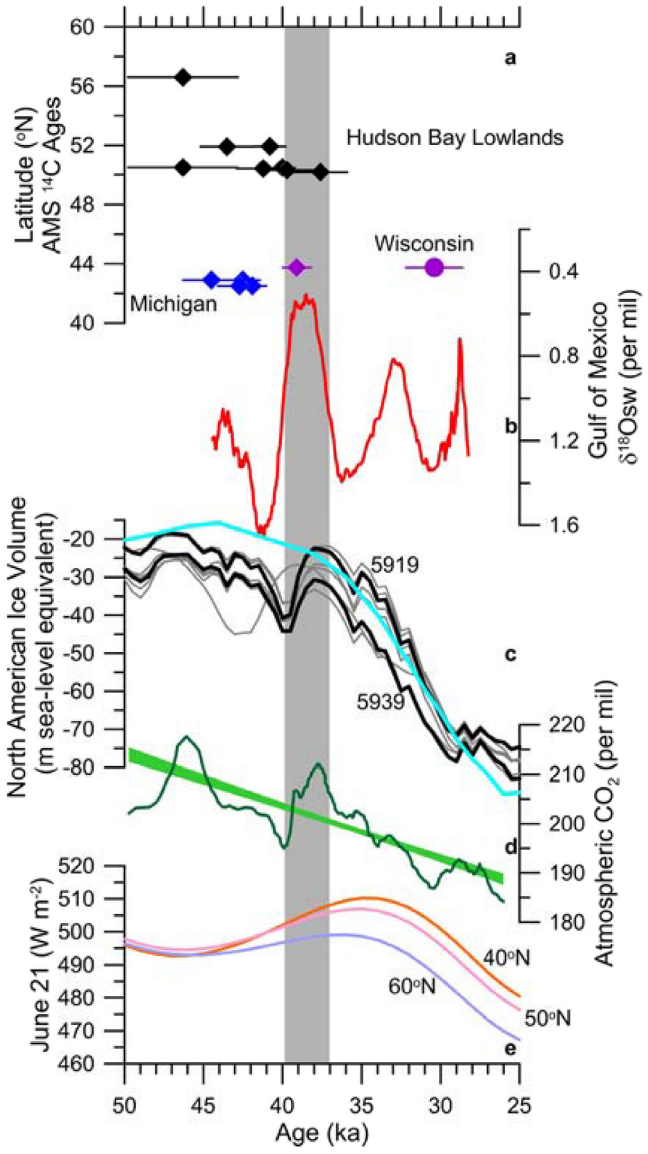

Fig. 2. Data and model results for MIS 3. (**a**) AMS ^{14}C ages from Wisconsin (purple), Michigan (blue; Monaghan et al., 1986; Colgan et al., 2015) and southernmost Hudson Bay lowland (black; Dalton et al., 2016); diamonds constrain the timing of Laurentide advance while the circle shows constraints on retreat. (**b**) Gulf of Mexico $\delta^{18}O_{sw}$ record with smoothing to a millennial timescale (Hill et al., 2006). (**c**) North American ice-sheet volume from Pico et al. (2017) in blue and Tarasov et al. (2012) in gray in global-mean sea-level equivalent volume; the latter matches AMS ^{14}C constraints in (**a**). The two simulations that match the Gulf of Mexico meltwater events in (**b**) are highlighted in black (5939 & 5919; see Fig. 3). (**d**) Atmospheric CO_2 concentration smoothed to a millennial timescale (dark green; Bereiter et al., 2015) with linear fit and 95% uncertainty window (light green). (**e**) Boreal summer (Laskar et al., 2004). (For interpretation of the references to color in this figure legend, the reader is referred to the Web version of this article.)

We use these two simulations (5919 & 5939) to define North American ice-sheet volume since ~45 ka (black lines in Fig. 2c). At 45 ka, the combined Laurentide, Cordilleran and Innuitian ice sheets contained 25–30 m GMSL, which grew to a maximum of 40–45 m GMSL by 40 ka. Ice volume then declined to a minimum of 23–30 m GMSL at 37 ka, with subsequent growth to 70–75 m GMSL by 30 ka. The rate of Laurentide ice-volume growth in run IDs 5919 & 5393 is 3.3–3.7 m GMSL ka^{-1} for 46–40 ka and 5.8–6.1 m GMSL ka^{-1} for 37–29 ka. For comparison, the overall deglacial rate

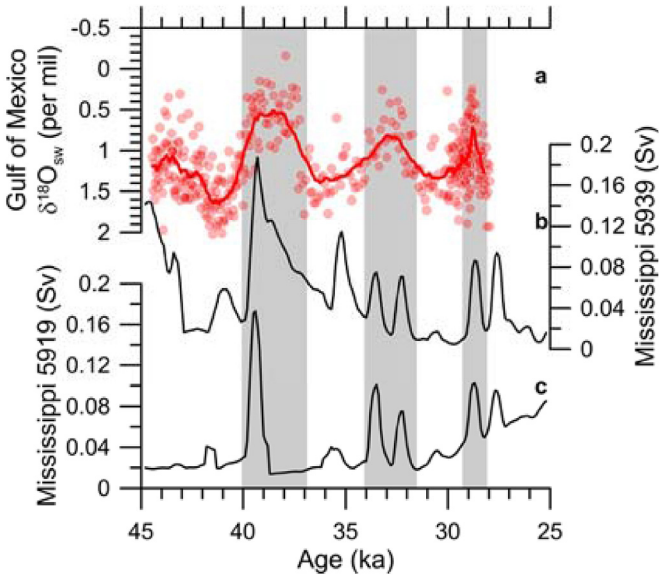

Fig. 3. Comparison of Gulf of Mexico $\delta^{18}O_{sw}$ records for MIS 3 (light red symbols, Hill et al., 2006) smoothed to a millennial timescale (red line) (**a**) with meltwater discharge to the Gulf of Mexico from the Tarasov et al. (2012) North American ice-sheet simulations 5939 (**b**) and 5919 (**c**) that match the timing of meltwater discharge in the geologic record (gray bars) in Sverdrups (Sv, $10^6\,m^3\,s^{-1}$). (For interpretation of the references to color in this figure legend, the reader is referred to the Web version of this article.)

of North American ice-volume loss in these simulations is 6–8 m GMSL ka^{-1}, which accelerated to 32–35 m GMSL ka^{-1} at 14.6–14.2 ka during meltwater pulse 1a (Deschamp et al., 2012).

4. Discussion and conclusions

With the Plymouth tills likely deposited by the Lake Michigan lobe, one would expect to find an equivalent till unit on the eastern side of Lake Michigan in western Michigan. Colgan et al. (2015) summarized the pre-LGM stratigraphy of western Michigan and suggested ice-free conditions until after ~29 ka. However, the youngest ^{14}C date constraining this range falls outside the ~17 ka Lake Michigan lobe limit and thus does not conflict with our findings. Indeed, four AMS ^{14}C ages below a pre-LGM till layer, which are within the 17-ka ice-margin extent, constrain a MIS 3 Lake Michigan lobe advance to after 41.9 ± 0.5 ka (Figs. 1 and 2a) (Monaghan et al., 1986; Colgan et al., 2015). Two conventional radiocarbon ages from above this Lake Michigan lobe till unit date the advance ending before 37.4 ± 2.3 ka, noting the added inherent uncertainty in conventional ^{14}C ages (Kehew et al., 2005; Colgan et al., 2015). Deposition of the Plymouth tills may also be concurrent with Superior lobe ice advance that resulted in the deposition of the Roxana loess in the Mississippi River valley after ~45 k (Fig. 1) (Clark et al., 1993; Syverson and Colgan, 2011; Muhs et al., 2018). Similarly, an advance of the Des Moines lobe into Iowa is ^{14}C dated to after ~41 ka that ended by ~29 ka (Fig. 1) (Kerr et al., 2017; Muhs et al., 2018).

Meltwater from the Lake Michigan, Superior and Des Moines lobes would drain through the Mississippi River into the Gulf of Mexico because the advance of the Lake Michigan lobe into Lake Michigan that we document would block eastward meltwater drainage via the lower Great Lakes forcing drainage southwards (Fig. 1) (e.g., Hansel and Mickelson, 1988; Licciardi et al., 1999). Our ^{14}C constraints for Plymouth tills deposition (along with the advance of the other ice lobes) is concurrent with decreased $\delta^{18}O_{sw}$ in the Gulf of Mexico that is interpreted to predominately record advance of the Laurentide ice sheet into the Mississippi River drainage basin and attendant addition of ^{18}O-depleted meltwater to the river (Fig. 2a and b) (Kennett and Shackleton, 1975; Leventer et al., 1982; Hill et al., 2006; Carlson, 2009; Williams et al., 2012; Wickert et al., 2013; Wickert, 2016; Vetter et al., 2017).

Southern Laurentide ice-sheet advance in the latter part of MIS 3 must have been rapid. Finite AMS ^{14}C dates from the southernmost Hudson Bay lowland (Dalton et al., 2016) suggest ice-free conditions up until ~40 ka (Fig. 1) (Skinner, 1973; Dredge and Thorliefson, 1987; Thorleifson et al., 1992; Allard et al., 2012; Dubé-Loubert et al., 2013). This is the region from which MIS 3 ice-flow indicators suggest ice advance to central Wisconsin and Michigan would be sourced (e.g., Thorleifson et al., 1992; Veillette et al., 1999; Kleman et al., 2010; Dubé-Loubert et al., 2013). The youngest MIS 3 AMS ^{14}C date from the southernmost Hudson Bay lowland is 37.6 ± 0.9 ka (Figs. 1 and 2a), which is consistent with our AMS ^{14}C date from the Plymouth tills of 39.1 ± 0.4 ka, when two sigma uncertainties are considered. One additional ^{14}C date from the southernmost Hudson Bay lowland is ~28.6 ka, but samples adjacent to this date yield infinite ^{14}C ages suggesting this sample is anomalous. The youngest robust AMS ^{14}C age from the southernmost Hudson Bay lowland and the older Plymouth tills age therefore imply minimum ice-margin advance rates of ~800 km ka^{-1} (2

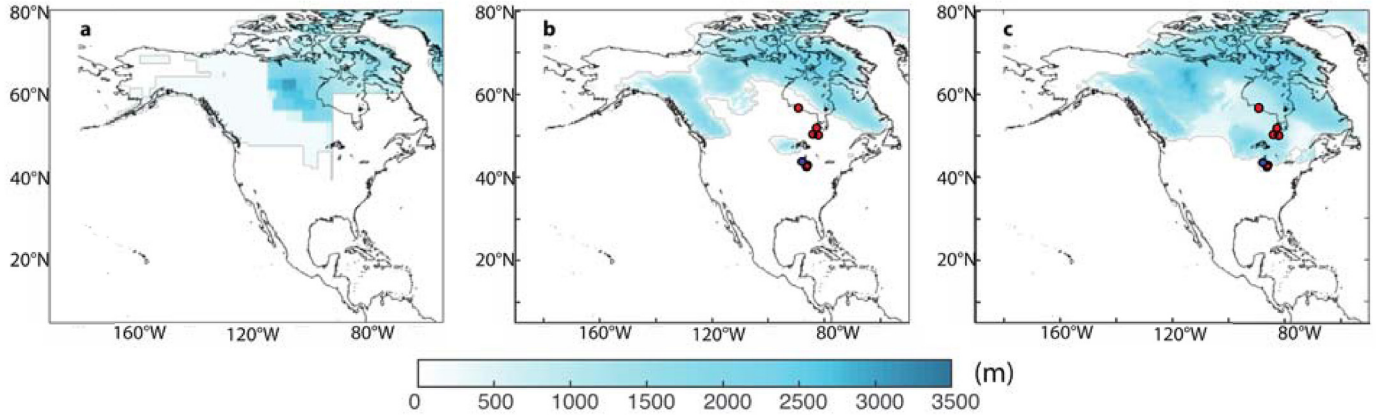

Fig. 4. Laurentide ice-sheet extent and thickness (color bar) at 44 ka in Pico et al. (2017) (**a**) and in the Tarasov et al. (2012) 5919 simulation (**b**). (**c**) The extent and thickness of 5919 at 40 ka (Tarasov et al., 2012). The locations of minimum-limiting ^{14}C dates (red) and the Wisconsin ^{14}C dates (blue) are indicated in (**b**) and (**c**). (For interpretation of the references to color in this figure legend, the reader is referred to the Web version of this article.)

sigma uncertainty) to ~400 km ka^{-1} (3 sigma uncertainty), which are of a similar magnitude as, but on average slower than, Laurentide ice-sheet retreat rates during its final deglaciation in the early Holocene (Ullman et al., 2016).

Pico et al. (2017) argued for a smaller Laurentide ice sheet during the early half of MIS 3 than is in earlier ice-history reconstructions (e.g., Lambeck et al., 2014). Using an approach adopting relative sea-level indicators along the U.S. mid-Atlantic, Pico et al. (2017) adopted a series of GIA models to infer the timing of major ice growth in the eastern sector of the Laurentide ice sheet. The anomalously high relative sea level recorded along the U.S. mid-Atlantic dated to mid-MIS 3 suggests a late growth of the peripheral bulge in this region, and thus a late growth of the southeastern Laurentide ice sheet, the region of ice loading to which the U.S. east coast is most sensitive. The proposed ice-loading history is consistent with an ice-free southernmost Hudson Bay lowland before ~40 ka (Fig. 4a), with the Laurentide ice sheet containing ~16 m GMSL at ~44 ka followed by rapid Laurentide ice-sheet growth to reach its LGM volume by ~26 ka (Fig. 2c) (Clark et al., 2009).

In Fig. 2c, we compare the Laurentide ice-volume evolution of 5919 & 5939 with the Laurentide ice-volume history of Pico et al. (2017). The two GMSL histories differ by < 20 m before 38 ka, with the Pico et al. (2017) falling between the 5919 & 5939 histories after 38 ka (Fig. 2c). In terms of ice extent before 40 ka (Fig. 4), there is disagreement on the amount of ice in the western Canadian Cordillera. However, east of ~120°W the two different approaches show a similar pattern with ice volume located mainly in the central to northern Hudson Bay and its lowland, which is consistent with geologic evidence for ice cover and deposition of rhythmites in the southernmost Hudson Bay lowland (e.g., Skinner, 1973; Dubé-Loubert et al., 2013). Both ice histories include a glaciated Hudson Strait (Fig. 4a and b), which would allow ice-sheet discharge of detrital carbonate during the Heinrich events of MIS 3 (e.g., Bond et al., 1992; Hemming, 2004; Channell et al., 2012). The 5919 ice-sheet model simulation has more extensive ice over eastern Labrador (Fig. 4b), which would agree with Laurentide ice-sheet erosion records from the Labrador Sea (e.g., Channell et al., 2012). Consequently, these ice-sheet model simulations provide support for the rapid ice growth inferred from the GIA model and U.S. east coast sea-level data (Pico et al., 2017), as they demonstrate the physical potential for rapid ice-sheet growth. Dredge and Thorleifson (1987) hypothesized that mid MIS 3 ice caps may have existed outside the contiguous Laurentide ice sheet, which the ice-sheet model also simulates (Fig. 4b). These local ice caps could promote such rapid ice-volume growth as these local ice caps can coalesce with the larger ice sheet as the latter expands (Fig. 4c) to the late MIS 3 extent of Dyke et al. (2002). While we use the term 'rapid growth', we note that the simulated growth of North American ice-sheet volume is still slower than the average and peak rates deglacial North American ice-volume loss (Tarasov et al., 2012).

We conclude by asking what forcing may have driven this MIS 3 advance of the southern Laurentide ice sheet. The advance of multiple southern Laurentide ice-sheet lobe after 40 ka suggests that the advance was a response to an external forcing mechanism, similar to the end of the LGM (Ullman et al., 2015). Pollen data from Iowa indicate the establishment of spruce by ~39 ka, which may extend to Illinois and Wisconsin, suggesting colder and wetter climate conditions that are conducive for ice-sheet growth (Clayton et al., 2001; Baker et al., 2015). We note that atmospheric CO_2 also declined on a multi-millennial timescale over MIS 3 (Fig. 2d) while boreal summer insolation increased 45–35 ka before dropping at the end of MIS 3 (in Fig. 2e we show June 21 intensity but a similar evolution is in the summer average). Nevertheless, what drove this colder and wetter climate, and potentially southern Laurentide ice-sheet advance, is difficult to discern at present and will require global climate model simulations across MIS 3 with transient changes in Earth's orbit and greenhouse gases, similar to what has been performed for the last deglaciation (e.g., Liu et al., 2009, 2012; He et al., 2013), that can be used to assess the potential forcing(s) of rapid Laurentide ice-sheet growth.

Acknowledgements

A.E.C. acknowledges support from the United States National Science Foundation. L.T. is supported by the Natural Sciences and Engineering Research Council of Canada. T.P. acknowledges support from United States National Science Foundation Graduate Research Fellowship Program and Harvard University. Comments by two anonymous reviewers improved an earlier version of this manuscript. This paper resulted from collaborations through the PALeo constraints on SEA level rise Past Global Changes working group and International Union for Quaternary Research international focus group.

Appendix A. Supplementary data

Supplementary data related to this article can be found at https://doi.org/10.1016/j.quascirev.2018.07.039.

References

Allard, G., Roy, M., Ghaleb, B., Richard, P.J.H., Larouche, A.C., Veillette, J.J., Parent, M., 2012. Constraining the age of the last interglacial-glacial transition in the Hudson Bay lowlands (Canada) using U-Th dating of buried wood. Quat. Geochronol. 7, 37–47.

Attig, J.W., Clayton, L., Mickelson, D.M., 1985. Correlation of late Wisconsin glacial phases in the western Great Lakes area. GSA Bulletin 96, 1585–1593.

Austermann, J., Mitrovica, J.X., Latychev, K., Milne, G.A., 2013. Barbados-based estimate of ice volume at Last Glacial Maximum affected by subducted plate. Nat. Geosci. https://doi.org/10.1038/NGEO1859.

Bajc, A.F., Karrow, P.F., Yansa, C.H., Curry, B.B., Nekola, J.C., Seymour, K.L., Mackie, G.L., 2015. Geology and paleoecology of a middle Wisconsin fossil occurrence in Zora Township, southwestern Ontario, Canada. Can. J. Earth Sci. 52, 386–404.

Baker, R.G., Bettis, E.A., Mandel, R.D., Dorale, J.A., Fredlund, G.G., 2015. Mid-wisconsinan environments on the eastern Great plains. Quat. Sci. Rev. 28, 873–889.

Bereiter, B., Eggleston, S., Schmitt, J., Nehrbass-Ahles, C., Stocker, T.F., Fischer, H., Kipstuhl, S., Chappellaz, J., 2015. Revision of the EPICA Dome C CO_2 record from 800 to 600 kyr before present. Geophys. Res. Lett. 42, 542–549.

Bond, G., Heinrich, H., Broecker, W., Labeyrie, L., McManus, J., Andrews, J., Huon, S., Jantschik, R., Clasen, S., Simet, C., Tedesco, K., Klas, M., Bonani, G., Ivy, S., 1992. Evidence for massive discharges of icebergs into the North Atlantic ocean during the last glacial period. Nature 360, 245–249.

Carlson, A.E., 2009. Geochemical constraints on the Laurentide ice sheet contribution to meltwater pulse 1A. Quat. Sci. Rev. 28, 1625–1630.

Carlson, A.E., Jenson, J.W., Clark, P.U., 2004. Field observations from the Tiskilwa till, IL and sky pilot till, MB of the Laurentide ice sheet. Géogr. Phys. Quaternaire 58, 229–239.

Carlson, A.E., Principato, S.M., Chapel, D.M., Mickelson, D.M., 2011. Quaternary geology of sheboygan county, Wisconsin. Wis. Geol. Nat. Hist. Surv. Bull. 106.

Channell, J.E.T., Hodell, D.A., Romero, O., Hillaire-Marcel, C., de Vernal, A., Stoner, J.S., Mazaud, A., Röhl, U., 2012. A 750-kyr detrital-layer stratigraphy for the North Atlantic (IODP sites U1302-U1303, Orphan Knoll, Labrador Sea). Earth Planet Sci. Lett. 317–318, 218–230.

Clark, P.U., Clague, J.J., Curry, B.B., Dreimanis, A., Hicock, S.R., Miller, G.H., Berger, G.W., Eyles, N., Lamothe, M., Miller, B.B., Mott, R.J., Oldale, R.N., Stea, R.R., Szabo, J.P., Thorleifson, L.H., Vincent, J.-S., 1993. Initiation and development of the Laurentide and Cordilleran ice sheets following the last interglaciation. Quat. Sci. Rev. 12, 79–114.

Clark, P.U., Dyke, A.S., Shakun, J.D., Carlson, A.E., Clark, J., Wohlfarth, B., Hostetler, S.W., Mitrovica, J.X., McCabe, A.M., 2009. The last glacial maximum. Science 325, 710–714.

Clayton, L., Attig, J.W., Mickelson, D.M., 2001. Effects of late Pleistocene permafrost on the landscape of Wisconsin, USA. Boreas 30, 173–188.

Colgan, P.M., Vanderlip, C.A., Braunschneider, K.N., 2015. Athens Subepisode (Wisconsin Episode) non-glacial and older glacial sediments in the subsurface of southwestern Michigan, USA. Quat. Res. 84, 382–397.

Dalton, A.S., Finkelstein, S.A., Barnett, P.J., Forman, S.L., 2016. Constraining the late pleistocene history of the Laurentide ice sheet by dating the Missinaibi

formation, Hudson Bay lowlands, Canada. Quat. Sci. Rev. 146, 288–299.
Deschamp, P., Durand, N., Bard, E., Hamelin, B., Camoin, G., Thomas, A., Henderson, G.M., Okuno, J., Yokoyama, Y., 2012. Ice-sheet collapse and sea-level rise at the Bølling warming 14,600 years ago. Nature 483, 559–564.
Dredge, L.A., Thorleifson, L.H., 1987. The middle Wisconsinan history of the Laurentide ice sheet. Géogr. Phys. Quaternaire 41, 215–235.
Dredge, L.A., Morgan, A.V., Nielsen, E., 1990. Sangamon and pre-sangamon interglaciations in the Hudson Bay lowlands of Manitoba. Géogr. Phys. Quaternaire 44, 319–336.
Dubé-Loubert, H., Roy, M., Allard, G., Lamothe, M., Veillette, J.J., 2013. Glacial and nonglacial events in the eastern James Bay lowlands, Canada. Can. J. Earth Sci. 50, 379–396.
Dyke, A.S., 2004. An Outline of North American Deglaciation with Emphasis on central and Northern Canada. Quaternary Glaciations-extent and Chronology, Part II, pp. 373–424.
Dyke, A.S., Andrews, J.T., Clark, P.U., England, J.H., Miller, G.H., Shaw, J., Veillette, J.J., 2002. The Laurentide and innuitian ice sheets during the last glacial maximum. Quat. Sci. Rev. 21, 9–31.
Hansel, A.K., Mickelson, D.M., 1988. A reevaluation of the timing and causes of high lake phases in the Lake Michigan basin. Quat. Res. 29, 113–128.
He, F., Shakun, J.D., Clark, P.U., Carlson, A.E., Liu, Z., Otto-Bliesner, B.L., Kutzbach, J.E., 2013. Northern Hemisphere forcing of Southern Hemisphere climate during the last deglaciation. Nature 494, 81–85.
Hemming, S.R., 2004. Heinrich events: massive late Pleistocene detritus layers of the North Atlantic and their global climate imprint. Rev. Geophys. 42 https://doi.org/10.1029/2003RG000128.
Hill, H.W., Flowers, B.P., Quinn, T.M., Hollander, D.J., Guilderson, T.P., 2006. Laurentide Ice Sheet meltwater and abrupt climate change during the last glaciation. Paleoceanography 21. https://doi.org/10.1029/2005PA001186.
Hughes, A.L.C., Gyllencreutz, R., Lohne, Ø.S., Mangerud, J., Svendsen, J.I., 2015. The last Eurasian ice sheets – a chronological database and time-slice reconstruction, DATED-1. Boreas. https://doi.org/10.1111/bor.12142.
Kehew, A.E., Beukema, S.P., Bird, B.C., Kozlowski, A.L., 2005. Fast flow of the Lake Michigan Lobe: evidence from sediment-landform assemblages in southwestern Michigan, USA. Quat. Sci. Rev. 24, 2335–2353.
Kennett, J.P., Shackleton, N.J., 1975. Laurentide ice sheet meltwater recorded in Gulf of Mexico deep-sea cores. Science 188, 147–150.
Kerr, P.J., Bettis, E.A., Tassier-Surine, S.A., Quade, D.J., Woida, K., Kilgore, S.M., 2017. Evidence for middle Wisconsin glaciation in North central Iowa. In: Geological Society of American Annual Meeting Abstract, 283-3.
Kleman, J., Jansson, K., De Angelis, H., Stroeven, A.P., Hättestrand, C., Alm, G., Glasser, N., 2010. North American Ice Sheet build-up during the last glacial cycle, 155-21 kyr. Quat. Sci. Rev. 29, 2036–2051.
Lambeck, K., Rouby, H., Purcell, A., Sun, Y., Sambridge, M., 2014. sea level and global ice volumes from the last glacial maximum to the Holocene. Proc. Natl. Acad. Sci. Unit. States Am. https://doi.org/10.1073/pnas.1411762111.
Laskar, J., Robutel, P., Joutel, F., Gastineau, M., Correia, A.C.M., Levrard, B., 2004. A long-term numerical solution for the insolation quantities of the Earth. Astron. Astrophys. 428, 201–285.
Leventer, A., Williams, D.F., Kennett, J.P., 1982. Dynamics of the Laurentide ice sheet during the last deglaciation: evidence from the Gulf of Mexico. Earth Planet Sci. Lett. 59, 11–17.
Licciardi, J.M., Teller, J.T., Clark, P.U., 1999. Freshwater Routing by the Laurentide Ice Sheet during the Last Deglaciation, 112. American Geophysical Union Monograph, pp. 177–201.
Lisiecki, L.E., Stern, J.V., 2016. Regional and global benthic $\delta^{18}O$ stacks for the last glacial cycle. Paleoceanography. https://doi.org/10.1002/2016PA003002.
Liu, Z., Carlson, A.E., He, F., Brady, E.C., Otto-Bliesner, B.L., Briegleb, B.P., Wehrenberg, M., Clark, P.U., Wu, S., Cheng, J., Zhang, J., Noone, D., Zhu, J., 2012. Younger dryas cooling and the Greenland climate response to CO_2. Proc. Natl. Acad. Sci. Unit. States Am. https://doi.org/10.1073/pnas.1202183109.
Liu, Z., Otto-Bliesner, B., He, F., Brady, E., Thomas, R., Clark, P.U., Carlson, A.E., Lynch-Stieglitz, J., Curry, W., Brook, E., Erickson, D., Jacob, R., Kutzbach, J., Chen, J., 2009. Transient climate simulation of last deglaciation with a new mechanism for Bølling-Allerød warming. Science 325, 310–314.
Maher, L.J., Mickelson, D.M., 1996. Palynological and radiocarbon evidence for deglaciation events in the green Bay lobe, Wisconsin. Quat. Res. 46, 251–259.
Monaghan, G.W., Larson, G.J., Gephart, G.D., 1986. Late wisconsinan drift stratigraphy of the Lake Michigan lobe in southwestern Michigan. GSA Bulletin 97, 329–334.
Muhs, D.R., Bettis III, E.A., Skipp, G.L., 2018. Geochemistry and mineralogy of late Quaternary loess in the upper Mississippi River valley, USA: provenance and correlation with Laurentide Ice Sheet history. Quat. Sci. Rev. 187, 235–269.
Nielsen, E., Morgan, A.V., Morgan, A., Mott, R.J., Rutter, N.W., Causse, C., 1986. Stratigraphy, paleoecology, and glacial history of the Gillam area, Manitoba. Can. J. Earth Sci. 23, 1641–1661.
Pico, T., Creveling, J.R., Mitrovica, J.X., 2017. sea-level records from the U.S. Mid-atlantic constrain Laurentide ice sheet extent during marine isotope stage 3. Nat. Commun. https://doi.org/10.1038/ncomms15612.
Pico, T., Mitrovica, J.S., Ferrier, K.L., Braun, J., 2016. Global ice volume during MIS 3 inferred from sea-level analysis of sedimentary core records in the Yellow River Delta. Quat. Sci. Rev. 152, 72–79.
Roy, M., 1998. Pleistocene Stratigraphy of the Lower Nelson River Area – Implications for the Evolution of the Hudson Bay lowland of Manitoba. Canada. M.Sc. Thesis, University of Québec, 220 p.
Siddall, M., Rohling, E.J., Thompson, W.G., Waelbroeck, C., 2008. Marine isotope stage 3 sea level fluctuations: data synthesis and new outlook. Rev. Geophys. 46 https://doi.org/10.1029/2007RG000226.
Skinner, R.G., 1973. Quaternary stratigraphy of the Moose river basin, Ontario. Geol. Surv. Can. Bull. 225, 77 p.
Stokes, C.R., Tarasov, L., Dyke, A.S., 2012. Dynamics of the North American ice sheet complex during its inception and build-up to the last glacial maximum. Quat. Sci. Rev. 50, 86–104.
Syverson, K.M., Colgan, P.M., 2011. The Quaternary of Wisconsin: an updated review of stratigraphy, glacial history and landforms. Dev. Quat. Sci. 15, 537–552.
Tarasov, L., Dyke, A.S., Neal, R.M., Peltier, W.R., 2012. A data-calibrated distribution of deglacial chronologies for the North American ice complex from glaciological modeling. Earth Planet Sci. Lett. 315–316, 30–40.
Thorleifson, L.H., Wyatt, P.H., Shilts, W.W., Nielsen, E., 1992. Hudson Bay lowland quaternary stratigraphy: evidence for early wisconsinan glaciation centered in quebec. In: Geological Society of America Special Paper, vol 270, pp. 207–220.
Ullman, D.J., Carlson, A.E., Hostetler, S.W., Clark, P.U., Cuzzone, J., Milne, G.A., Winsor, K., Caffee, M., 2016. Final Laurentide ice-sheet deglaciation and Holocene climate-sea level change. Quat. Sci. Rev. 152, 49–59.
Ullman, D.J., Carlson, A.E., LeGrande, A.N., Moore, A.K., Anslow, F.S., Caffee, M., Syverson, K.M., Licciardi, J.M., 2015. Southern Laurentide ice-sheet retreat synchronous with rising boreal summer insolation. Geology 43, 23–26.
Veillette, J.J., Dyke, A.S., Roy, M., 1999. Ice-flow evolution of the labrador sector of the Laurentide ice sheet: a review, with new evidence from northern quebec. Quat. Sci. Rev. 18, 993–1019.
Vetter, L., Spero, H.J., Eggins, S.M., Williams, C., Flower, B.P., 2017. Oxygen isotope geochemistry of Laurentide ice-sheet meltwater across Termination I. Quat. Sci. Rev. 178, 102–117.
Wickert, A.D., 2016. Reconstruction of North American drainage basins and river discharge since the last glacial maximum. Earth Surf. Dynam. 4, 831–869.
Wickert, A.D., Mitrovica, J.X., Williams, C., Anderson, R.S., 2013. Gradual demise of a thin southern Laurentide ice sheet recorded by Mississippi drainage. Nature 502, 668–671.
Williams, C., Flower, B.P., Hasting, D.W., 2012. Seasonal Laurentide ice sheet melting during the “Mystery interval” (17.5-14.5 ka). Geology 40, 955–958.